Calpain inhibitor MDL28170 alleviates cerebral ischemia-reperfusion injury by suppressing inflammation and autophagy in a rat model of cardiac arrest

WEN-YAN WANG[1*], JIA-XIN SHI[2*], MENG-HUA CHEN[2], XIANG-ZHEN ZHUGE[3], CHUN-GUANG DAI[1] and LU XIE[3]

[1]Intensive Care Unit, The Affiliated Hospital of Guilin Medical University, Guilin, Guangxi Zhuang Autonomous Region 541001; [2]Department of Cardiology, Foresea Life Insurance Nanning Hospital; [3]Department of Physiology, Guangxi Medical University, Nanning, Guangxi Zhuang Autonomous Region 530000, P.R. China

Received July 8, 2022; Accepted February 20, 2023

DOI: 10.3892/etm.2023.11895

Abstract. Cerebral ischemia-reperfusion injury (CIRI) is associated with a poor neurological prognosis in patients who have experienced cardiac arrest (CA) and cardiopulmonary resuscitation (CPR). The aim of the current study was to investigate the potential role of a calpain inhibitor in CIRI using a rat model of CA. CA was induced in adult male Sprague-Dawley rats, and MDL28170 (a calpain inhibitor) was administered to the rats within 30 min after the return of spontaneous circulation. Differences between groups were evaluated by measuring survival rate, CPR duration and neurological deficit score. Hematoxylin-eosin staining and Nissl staining were performed to assess cerebral injury, and microstructure and autophagy were assessed by transmission electron microscopy. The levels of calpain-1, calpain-2, calpastatin, interleukin (IL)-1β, tumor necrosis factor (TNF)-α, P62, beclin-1 and LC3 in the brain tissues were determined using western blotting and double immunofluorescence staining. There was no significant difference in CPR duration or survival rate among the groups. At 24 h after CPR, the CA group demonstrated damaged tissue morphology; decreased neurological deficit scores, and P62 expression; and upregulated calpain-2, IL-1βp17, TNF-α, beclin-1 and LC3 levels in the cortex. However, MDL28170 improved neuronal function and suppressed inflammation and autophagy by inhibiting calpain-2 level, but there were no differences in the calpain-1 and calpastatin levels. These results suggest that calpain-2, inflammation and autophagy are involved in CA-induced CIRI. MDL28170 inhibited calpain-2 expression, inflammation and autophagy, which suggests its potential efficacy in treating post-CA nerve damage.

Introduction

The morbidity and mortality associated with cardiac arrest (CA) are high worldwide, and the return of spontaneous circulation (ROSC) causes severe cerebral ischemia-reperfusion injury (CIRI), which is the main cause of coma in patients with CA (1,2). Owing to the complex mechanism of CIRI, the available therapies are not ideal to promote nervous system recovery (3). Therefore, the development of new strategies for the clinical management of CIRI following CA and cardiopulmonary resuscitation (CPR) has been a challenge.

During CIRI, the fluidity of the mitochondrial membrane decreases, and the synthesis of adenosine triphosphate is reduced (4,5). Additionally, the ability of the plasma membrane and endoplasmic reticulum (ER) calcium pumps to control calcium levels is compromised, which leads to intracellular calcium overloads (6,7). Persistent calcium overloads lead to excessive activation of calpain, which activates or hydrolyzes other enzymes, resulting in further damage to neuronal function (8). Therefore, the development of methods to alleviate CIRI by blocking cellular dysfunction caused by calpain activation represents an active area of research (9).

Calpain, a neutral cysteine protease, is widely expressed in several organisms (humans, fish and amphibians). The calpain protein family includes >10 subtypes (CAPN1-3, 5-15 and 17), but calpain-1 and calpain-2 are of particular interest because they are highly expressed in the brain tissue and show calcium-dependent activities (10,11). Animal experiments have shown that calpain plays a key role in the pathophysiology

Correspondence to: Professor Lu Xie, Department of Physiology, Guangxi Medical University, 22 Shuangyong Road, Qingxiu, Nanning, Guangxi Zhuang Autonomous Region 530000, P.R. China
E-mail: xielu8282@163.com

*Contributed equally

Abbreviations: CA, cardiac arrest; CIRI, cerebral ischemia-reperfusion injury; CPR, cardiopulmonary resuscitation; DMSO, dimethyl sulfoxide; NS, normal saline; ER, endoplasmic reticulum; GAPDH, glyceraldehyde 3-phosphate dehydrogenase; HE, hematoxylin-eosin; IL, interleukin; NDS, neurological deficit score; ROSC, return of spontaneous circulation; TEM, transmission electron microscopy; TNF, tumor necrosis factor

Key words: cardiopulmonary resuscitation, MDL28170, calpain-2, inflammation, autophagy, cerebral ischemia-reperfusion

of cerebral ischemic injury (12,13). Calpastatin (encoded by CAST) is an endogenous specific inhibitor of calpain and acts on both calpain-1 and calpain-2 (14). After a cerebral ischemic injury, the calpastatin level is not adequate to counterbalance excessively activated calpain (15). Therefore, exogenous calpain inhibitors have been developed to alleviate ischemic brain injury, brain trauma and other neurological diseases (16). MDL28170 is a non-selective calpain inhibitor (17,18) that exerts a neuroprotective effect on cerebral ischemia and hypoxic injury in adult and neonatal rats by inhibiting calpain-1 (19).

In 1998, Li *et al* (20) revealed that post-ischemic treatment with the calpain inhibitor MDL28170 (in a study on bilateral common carotid artery occlusion-induced global cerebral ischemia-reperfusion injury) improved brain damage in the gerbil model of systemic ischemia; however, apart from the inhibition of calpain-induced proteolysis, other mechanisms are unclear. Furthermore, MDL28170 can reduce traumatic brain injury in rats by blocking calpain-2 (18). It is well known that the inflammatory response plays an important role in CIRI (21). When cerebral ischemia occurs, the immune system is triggered, immune cells in the brain tissue are activated and inflammatory cytokines [such as interleukin (IL)-1β and tumor necrosis factor (TNF)-α] are released. A large number of inflammatory factors invade the brain parenchymal tissue and disrupt the blood-brain barrier. It also stimulates the synthesis of other immune cells and adhesion molecules in the blood, amplifying the inflammatory cascade and ultimately exacerbating nerve damage (22). In a study on a traumatic brain injury mouse model, MDL28170 played a neuroprotective role by reducing the expression of NF-κB and decreasing the release of IL-1β and TNF-α (23). Our previous research on brain injury after cardiac arrest in the same period demonstrated that calpain-2 is closely associated with neuroinflammation induced by brain astrocytes and microglia (24), but the role of different calpain isoforms in brain injury is unclear. Therefore, it would be beneficial to explore the changes of inflammatory response in CIRI by targeting calpain.

Autophagy is an important intracellular self-degradation process; however, excessive autophagy can lead to cell component depletion and cell death. Increasing evidence suggests that autophagy is involved in CIRI (25,26). Our previous study demonstrated that the inhibition of mitochondrial autophagy can attenuate the brain damage in rats after CA and CPR (27). Moreover, a recent study showed that calpain-2 is involved in TNF-α-mediated hippocampal neuron autophagy, resulting in neuronal death (28). To the best of our knowledge, the present study is the first to evaluate calpain-related proteins and the effect of MDL28170 on inflammation and autophagy in CIRI by constructing a CA rat model through retroesophageal electrical stimulation.

Materials and methods

Animals. A total of 81 male Sprague-Dawley rats (8-10-week-old; body weight, 220-250 g; Experimental Animal Center of Guangxi Medical University, Nanning, China) were used in the present study. The rats were housed in facilities with a 12 h/12 h light/dark cycle at 25˚C and had access to food and water *ad libitum*. All animal procedures were conducted in compliance with the Guide for the Care and Use of Experimental Animals. The study was approved by the Animal Ethics Committee of Guangxi Medical University (Nanning, China; approval no. 20190915). Except for 21 rats that died during CA-CPR modeling, all other rats were euthanized with 2% pentobarbital sodium (90 mg/kg) as well as via cervical dislocation at 24 h after CA/CPR; the duration of the experiment was 24 h. There were two main causes of mortality in the animals: i) The rats failed to be resuscitated after cardiac arrest induced during the experiment; or ii) at the end of the experiment, the rats were euthanized. The vital signs (body temperature, heart rate and blood pressure) of the rats were continuously monitored during the entire processes of model-making and euthanasia. Rat mortality was confirmed when the following four signs were found: Lack of a heartbeat; lack of respiration; lack of corneal reflex; and presence of rigor mortis.

Experimental CA/CPR model. All rats were subjected to fasting for 12 h before surgery. Anesthesia was induced with an intraperitoneal injection of 2% pentobarbital sodium (30 mg/kg). CA was induced by electrical stimulation with transesophageal cardiac pacing, as described previously (29). Before CA induction, femoral artery blood pressure monitoring, femoral venipuncture catheterization and endotracheal intubation were performed. After 7 min of untreated CA, CPR was performed by manual chest compression (180 compressions/min) to a depth of 25-30% of the anteroposterior diameter of the thorax and with equal compression-relaxation duration by the same investigator. ROSC was defined as an unassisted pulse with a mean arterial pressure of ≥50 mmHg for ≥1 min. When the blood pressure and autonomous respiration were stable (breaths ≥40/min), mechanical ventilation was withdrawn after ROSC.

Drug treatment and experimental groups. MDL28170, a calpain inhibitor (cat. no. M6690; Sigma-Aldrich; Merck KGaA), was dissolved in 8% dimethyl sulfoxide (DMSO) to final concentrations of 1.5 and 3.0 mg/kg (30). The vehicle group received an equal volume of solvent via the same method of administration.

Successfully established model rats were randomly divided into four groups: i) CA control group, normal saline (NS) was administered (NS, n=18); ii) control vehicle group, 8% DMSO was administered (DMSO, n=18); iii) low-dose MDL28170 group (MDL-l, 1.5 mg/kg, n=18); and iv) high-dose MDL28170 group (MDL-h, 3.0 mg/kg, n=18). Another nine rats were selected for the sham operation group, which were subjected to the same procedures but without CA and CPR. All drugs were injected into the left femoral vein within 30 min of ROSC.

Evaluation of survival rate, neurological deficit score (NDS) and CPR duration. CPR duration was measured as the time from the start of cardiac compression to the ROSC. The survival rate and NDS of the experimental rats were evaluated 24 h after the ROSC by an investigator blinded to the experimental groups. NDS was graded on a scale of 0-80 based on the arousal, reflex, motor, sensory and balance responses (most severe deficit, 0; normal performance, 80) (31). All experimental rats were used for the subsequent tests to evaluate neuronal function.

Tissue sampling and preparation. Three experimental animals from each group were deeply anesthetized using 2% pentobarbital sodium (90 mg/kg) at 24 h after CA/CPR. Saline and 4% paraformaldehyde were infused through the aorta for 2 h at 4˚C. The excised brain tissue was immediately fixed in 10% paraformaldehyde at room temperature for 48 h, and paraffin-embedded sections were prepared. Thus, 3-μm-thick paraffin-embedded sections were used for hematoxylin-eosin (HE) or double immunofluorescence staining, and 5-μm-thick paraffin-embedded sections for Nissl staining as detailed below.

HE and Nissl staining. The prepared brain sections were dehydrated in the xylene solution to remove the paraffin, then rehydrated in a descending alcohol series (100, 95, 75 and 50% ethanol) at 25˚C for 5 min/step. Tissue samples were stained with hematoxylin at 25˚C for 5 min. The tissue samples were stained with HE and 1% hydrochloric acid in 70% ethanol at 25˚C for 5 min. The specimens were then dried, covered with cover slides and observed under an optical microscope (Olympus Corporation).

For Nissl staining, the prepared brain sections also were dehydrated in the xylene solution to remove the paraffin and then rehydrated in a descending alcohol series (100, 95, 75 and 50% ethanol) at 25˚C for 5 min/step. Tissue samples were stained with toluidine blue solution (cat. no. G3668; Beijing Solarbio Science & Technology Co., Ltd.) in a dark, airtight container at 70% humidity and 60˚C for 30 min. Samples were then re-dyed in 0.5% eosin at 25˚C for 3 sec. Under a light microscope, the Nissl bodies in the tissue sections were counted in five randomly selected regions of every sample using ImageJ version 1.46 (National Institutes of Health).

Transmission electron microscopy (TEM) analysis. Three rats from each group were used for TEM analysis. After cerebral perfusion with 4% paraformaldehyde, 40 mg of the cortex specimen was placed in 2.5% glutaraldehyde and stored at 4˚C for 24 h. The samples were fixed with 1% osmium tetroxide at room temperature for 3 h, dehydrated in ethanol and then embedded in epoxy resin at 37˚C for 1 h. According to the standard operating principles of three-dimensional localization, resin blocks were cut into ultrathin slices (100-nm), fixed on metal mesh grids and double-stained using lead citrate and uranyl acetate at 25˚C for 30 min. Finally, the morphology of the neurons was observed using TEM. The images were recorded and viewed with an H-7650 TEM unit (Hitachi, Ltd.).

Western blotting. Rats (n=3 per group) were euthanized after deep anesthetization, and the brain tissue was immediately excised and washed with cold saline. The isolated cerebral cortex was quick-frozen in liquid nitrogen (-196˚C) for 3 h and stored at -80˚C for subsequent western blotting. The cortex sample (50 mg from each group) was lysed at 4˚C, and the tissue homogenate was centrifuged at 13,000 x g for 15 min at 4˚C to extract the proteins. A bicinchoninic acid protein assay kit (cat. no. P0012; Beyotime Institute of Biotechnology) was used to test the total protein concentration. Protein samples (40 μg/lane) were separated using sodium dodecyl sulfate-polyacrylamide gel (12, 10 or 8% separation gel) electrophoresis and transferred onto a polyvinylidene fluoride membrane (pore size, 0.2 μm; MilliporeSigma), which was blocked for 1 h with 5% fat-free milk solution at 25˚C and incubated with the corresponding primary antibodies overnight at 4˚C. The following rabbit anti-rat primary antibodies were used: Calpain-1 (1:1,000; cat. no. ab28258; Abcam), calpain-2 (1:1,000; cat. no. 11472-1-AP; Wuhan Sanying Biotechnology, Inc.), calpastatin (1:5,000; cat. no. ab226249; Abcam), P62 (1:1,000; cat. no. #5114; Cell Signaling Technology, Inc.), Beclin-1 (1:1,000; cat. no. #3495; Cell Signaling Technology, Inc.), LC3 (1:2,000; cat. no. ab192890; Abcam), IL-1β (1:100; cat. no. sc-32294; Santa Cruz Biotechnology, Inc.), TNF-α (1:1,000; cat. no. ab6671; Abcam) and glyceraldehyde 3-phosphate dehydrogenase (GAPDH; 1:1,000; cat. no. #5174; Cell Signaling Technology, Inc.). After washing with Tris-buffered saline with 0.2% Tween 20, the samples were incubated with a goat anti-rabbit IgG fluorescence-labeled secondary antibody (1:20,000; cat. no. #5151T; Cell Signaling Technology, Inc.) at 25˚C for 1 h. Finally, the strip density was detected using the Tanon™ High-sig ECL Western Blotting Substrate (Guangzhou Yuwei Biotechnology Instrument Co., Ltd.). ImageJ version 1.46 (National Institutes of Health) was used to quantify each protein band, with measured levels normalized to that of GAPDH.

Double immunofluorescence staining. The brain tissue sections were dewaxed, hydrated in a descending alcohol series (100, 95, 75 and 50% ethanol), and microwaved at 60˚C for 5 min in an ethylenediaminetetraacetic acid antigen-repair buffer (pH 8.0; Beyotime Institute of Biotechnology), followed by incubation at 25˚C for 20 min in phosphate-buffered saline (pH 7.4) containing 0.3% Triton X-100 (phosphate-buffered saline with Tween 20). The tissue sections were blocked in normal goat serum at 25˚C for 30 min (OriGene Technologies, Inc.) with bovine serum albumin (Thermo Fisher Scientific, Inc.). The specimens were initially incubated at 4˚C with rabbit polyclonal anti-calpain-2 (1:2,000; cat. no. 11472-1-AP; ProteinTech Group, Inc.). The samples were stored at 4˚C and incubated overnight. The following day, the sections were incubated with horseradish peroxidase-conjugated goat anti-rabbit secondary antibody (1:500; cat. no. GB23301; Wuhan Servicebio Technology Co., Ltd.) in the dark at 25˚C for 60 min. Next, the fluorescein isothiocyanate reagent was added and the sections were incubated for 10 min in dark at 25˚C. Subsequently, the sections were placed in a repair box filled with citric acid (pH 6.0) antigen-repair solution and heated in a microwave oven (heated at 70˚C for 8 min, no heat for 10 min, heated at 60˚C for 7 min and then allowed to gradually cool down). The sections were incubated with rabbit monoclonal anti-LC3 (1:1,000; cat. no. ab192890; Abcam) overnight at 4˚C. Next, the brain tissue was incubated with Cy3-coupled secondary antibody solution (1:300; cat. no. GB21303; Wuhan Servicebio Technology Co., Ltd.) at 25˚C for 60 min, followed by incubation with DAPI at 25˚C for 10 min. Finally, an auto-fluorescence quenching agent was added to avoid background fluorescence and the fluorescent markers were observed. The slides were scanned using the Pannoramic DESK system (3DHISTECH Kft.) for panoramic scanning. Full-field digital slice images were generated, and the CaseViewer Windows application (3DHISTECH Kft.) was used to compile them. Finally, ImageJ version 1.46 (National Institutes of Health) was used to analyze the rates of cells positive for calpain-2 and LC3 and the ratio of calpain-2 to LC3 in the cells.

Table I. Survival rate, CPR duration and NDS in each group.

Group	Survival rate, n (%)	n	CPR duration, sec	NDS, median (25th percentile, 75th percentile)
Sham	9/9 (100.0)	9	-	80 (80, 80)
NS	11/18 (61.1)	11	98.36±3.331	70 (69, 71)[a]
DMSO	12/18 (66.7)	12	92.25±1.733	70 (68, 71.75)[a]
MDL-l	13/18 (72.2)	13	94.85±1.996	73 (70, 74)[a]
MDL-h	15/18 (83.3)	15	93.53±2.24	74 (72, 76)[a,b,c]

[a]P<0.001 vs. Sham; [b]P<0.05 vs. NS; [c]P<0.05 vs. DMSO. CPR, cardiopulmonary resuscitation; NDS, neurological deficit score; NS, 0.9% saline group; DMSO, 8% dimethyl sulfoxide group; MDL, MDL28170; l, low; h, high.

Statistical analysis. GraphPad Prism 7 (GraphPad Software, Inc.) was used for all statistical analyses and graph creation. The assumptions of normality were evaluated using Shapiro-Wilk test. Statistical differences between groups were analyzed using a one-way analysis of variance and Tukey's post hoc test. The non-normally distributed data and the intergroup comparisons were evaluated using the Kruskal-Wallis test and Dunn's test. P<0.05 was considered to indicate a statistically significant difference. The survival rates were analyzed using a χ^2 cross-table. The NDS is expressed as median and interquartile range, and other data are presented as mean ± standard deviation.

Results

Survival rate, CPR duration and NDS. There were no significant differences in the CPR duration among the groups (P>0.05; Table I). The survival rate of rats in the sham group was 100%. The survival rate of rats in the 0.9% saline (NS) (61.1%), DMSO (66.7%), MDL-l (72.2%) and MDL-h (83.3%) groups was lower compared with that of rats in the sham group, but no significant difference was found in the survival rate among the groups (P>0.05; Table I). Additionally, the NDS of the NS (70), DMSO (70), MDL-l (73) and MDL-h (74) groups was significantly lower compared with that of the sham group (80) (all P<0.05). However, the NDS of the MDL-h group was significantly higher compared with that of the NS and DMSO groups (P<0.05; Table I).

Morphological changes in neurons in the cortex after CA and CPR. To evaluate the effect of different doses of the calpain inhibitor MDL28170 on CIRI after CPR, morphological changes in neurons were observed using HE and Nissl staining. As shown in the HE-stained images, the nuclei of cells in the sham group were round and intact, the nucleoli were visible, and the fiber structure of the brain tissue was normal. In the NS and DMSO groups, necrotic cells, nuclear deformation and pyknosis, cell vacuoles and tissue exudation were observed. The morphology of the cortical neurons in the MDL-l and MDL-h groups was improved compared with that in the NS and DMSO groups, and the morphology of the cortical neurons in the MDL-h group was improved compared with that in any other group (Fig. 1A). Nissl staining revealed significantly fewer Nissl bodies in the model groups compared with in the sham group (P<0.05; Fig. 1B and C). The numbers of Nissl bodies were significantly increased in the MDL-h group compared with in the NS and DMSO groups (P<0.05; Fig. 1B and C).

Expression of calpastatin, calpain-1 and calpain-2 in the cortex after CA and CPR. Western blotting of calpastatin, calpain-1 and calpain-2 revealed no significant differences in the level of calpastatin or calpain-1 among the groups (Fig. 2A-C). However, the expression of calpain-2 in the NS and DMSO groups was significantly higher compared with that in the sham group (P<0.05; Fig. 2A and D). The MDL-h group, which was treated with 3.0 mg/kg of MDL28170, showed a significantly lower level of calpain-2 compared with the NS and DMSO groups (P<0.05; Fig. 2A and D).

Expression of IL-1β and TNF-α in the cortex after CA and CPR. Western blotting of ProIL-1β (precursor IL-1β) showed no significant differences among the groups (P>0.05) (Fig. 3A and B). The expression of IL-1βp17 (mature IL-1β) and TNF-α in the NS, DMSO and MDL-L groups was significantly higher compared with that in the sham group (P<0.05; Fig. 3A, C and D). However, the expression of IL-1βp17 (mature IL-1β) and TNF-α in the MDL-h group was significantly lower compared with that in the NS and DMSO groups (P<0.05; Fig. 3A, C and D).

Characterization of ultrastructural changes and autophagy by TEM. A comparison of the ultrastructural changes in the cerebral cortex in the sham, NS and MDL-h groups, as determined by TEM, showed the effect of MDL28170 on autophagy after the inhibition of calpain-2. In the sham group, the nucleus was round, and the nuclear membrane was continuous and intact. In the NS and MDL-h groups, the size of the nucleus changed, the ER and mitochondria were dilated, and vacuolar degeneration was observed (Fig. 4A and B). The damage to neurons in the NS group was more severe compared with that to neurons in the MDL-h group, and autophagy was detected at every stage in the NS group (Fig. 4C).

Expression of P62, beclin-1 and LC3 in the cortex after CA and CPR. To determine the effect of MDL28170 on autophagy-related proteins after the inhibition of calpain-2, P62, beclin-1 and LC3 expression levels were detected in the cortex of rats in the sham, NS and MDL-h groups by western

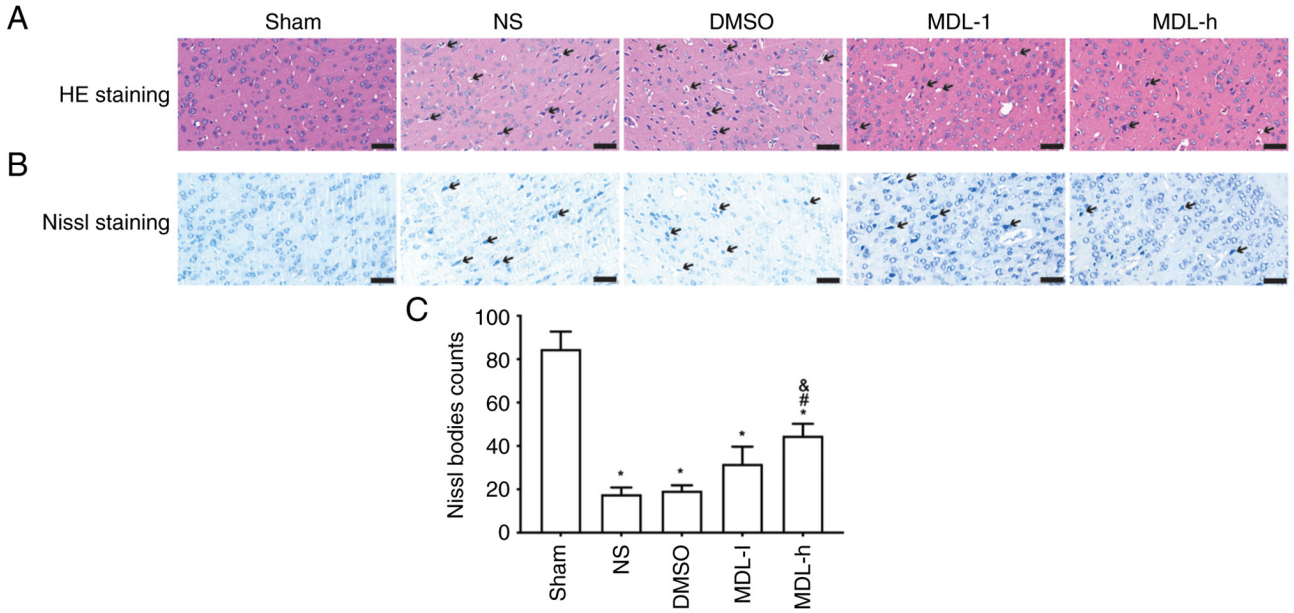

Figure 1. HE staining and Nissl staining of the cerebral cortex in rats 24 h post-CA/cardiopulmonary resuscitation. (A) HE staining of the cerebral cortex. Dead and vacuolar cells are shown by black arrows (scale bar, 50 μm). (B) Nissl staining of the cerebral cortex. Dead and vacuolar cells are shown by black arrows (scale bar, 50 μm). (C) Column chart shows a comparison of the number of Nissl bodies in each group. (n=3). *P<0.05 vs. the sham group; $^{\#}$P<0.05 vs. the NS group; $^{\&}$P<0.05 vs. the DMSO group. HE, hemoxylin and eosin; CA, cardiac arrest; CPR, cardiopulmonary resuscitation; NS, normal saline; MDL-l, low-dose MDL28170 group; MDL-h, high-dose MDL28170 group.

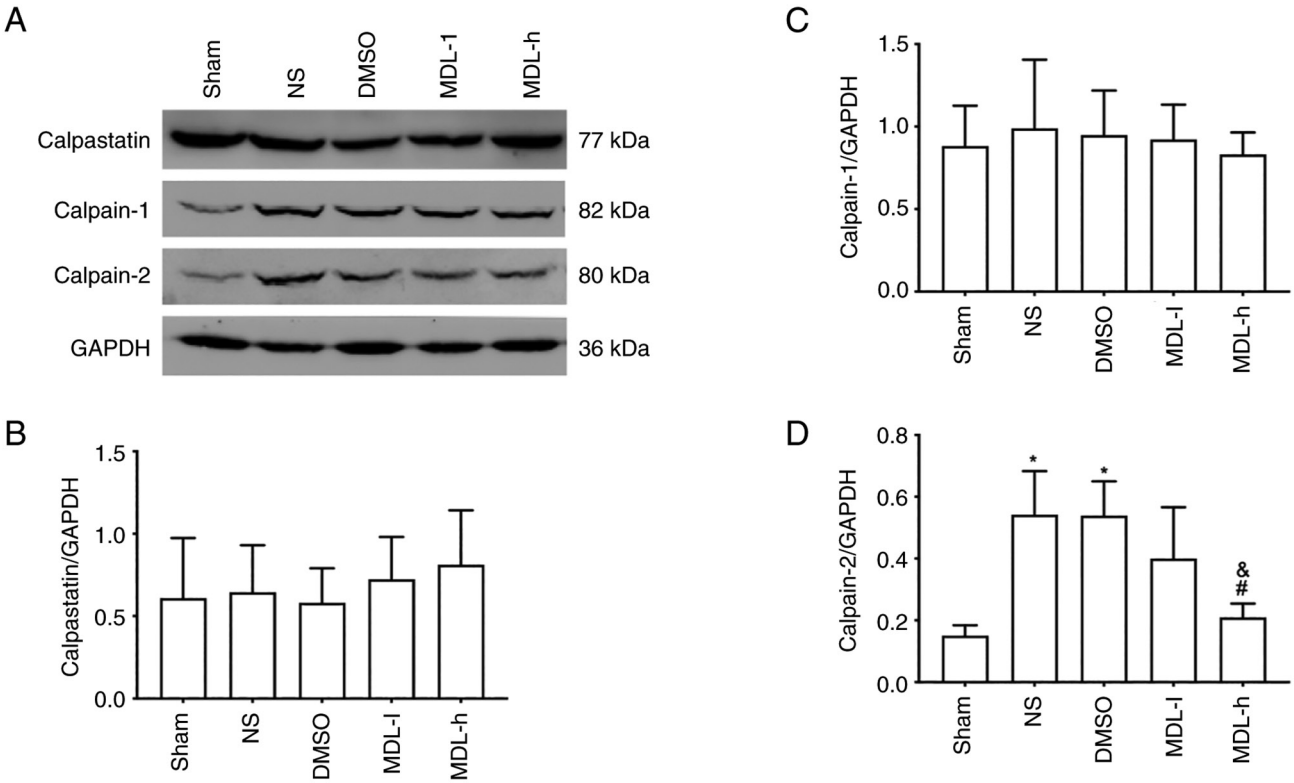

Figure 2. Western blotting analysis for calpastatin, calpain-1 and calpain-2. (A) Representative western blots of calpastatin, calpain-1 and calpain-2. (B) Western blotting analysis of calpastatin. (C) Western blotting analysis of calpain-1. (D) Western blotting analysis of calpain-2. Band intensities were normalized to those of GAPDH. (n=3). *P<0.05 vs. the sham group; $^{\#}$P<0.05 vs. the NS group; $^{\&}$P<0.05 vs. the DMSO group. NS, normal saline; MDL-l, low-dose MDL28170 group; MDL-h, high-dose MDL28170 group.

blotting at 24 h following CA and CPR. As shown in Fig. 5, the levels of beclin-1 and LC3I/LC3II were significantly upregulated in the NS group compared with that in the sham group. Additionally, the LC3I/LC3II level in rats in the MDL-h group was significantly higher compared with that in rats in the sham group, suggesting that autophagy increased after CIRI. When

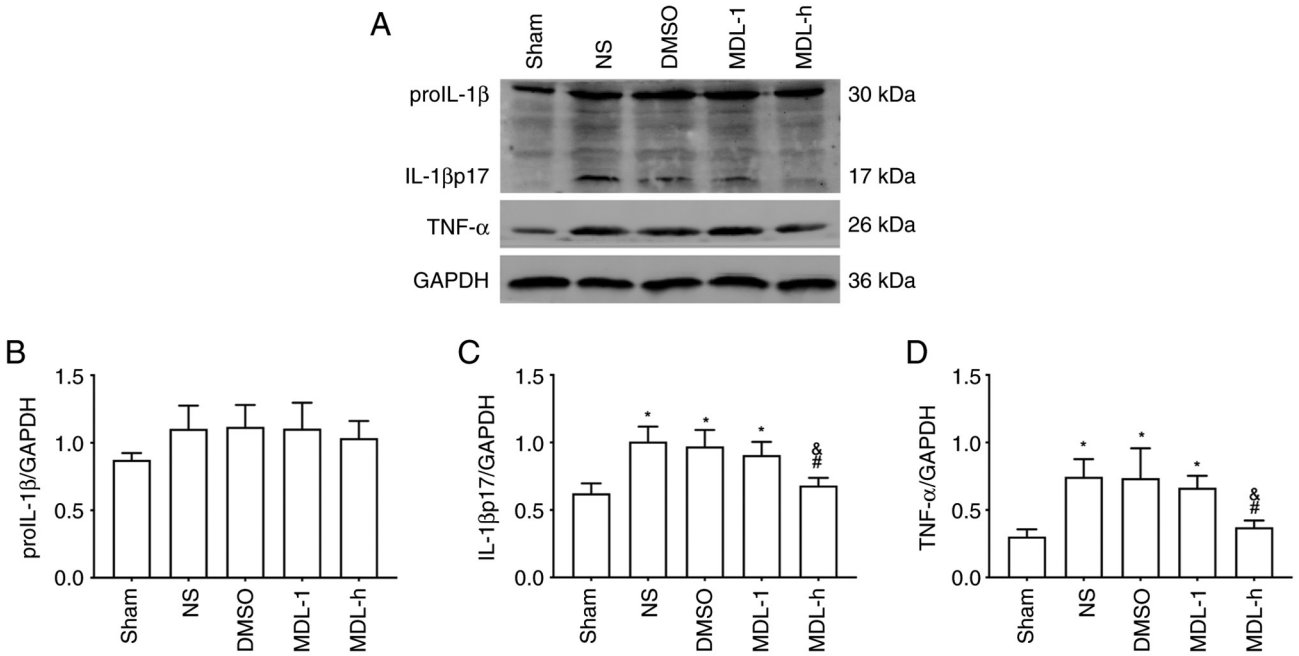

Figure 3. Western blotting analysis for IL-1β and TNF-α. (A) Representative western blots of IL-1β and TNF-α. (B) Western blotting analysis of proIL-1β. (C) Western blotting analysis of IL-1βp17. (D) Western blotting analysis of TNF-α. Band intensities were normalized to those of GAPDH. (n=3). *P<0.05 vs. the sham group; #P<0.05 vs. the NS group; &P<0.05 vs. the DMSO group. proIL-1β, precursor IL-1β; IL-1βp17, mature IL-1β; NS, normal saline; MDL-l, low-dose MDL28170 group; MDL-h, high-dose MDL28170 group.

MDL28170 was administered to rats in the MDL-h group, the levels of beclin-1 and LC3I/LC3II decreased, whereas that of P62 increased compared with the levels in rats in the NS group (P<0.05; Fig. 5).

Double immunofluorescence staining of calpain-2 and LC3 in the cortex following CA and CPR. To clarify the association between calpain-2 and autophagy, the co-localization of calpain-2 and LC3 in the sham, NS and MDL-h groups was examined by double immunofluorescence staining. As shown in Fig. 6A-C, the rate of cells positive for calpain-2 and LC3 in the NS group was significantly higher compared with that in the sham group, whereas the positivity rate of cells in the MDL-h group was significantly lower compared with that in the NS group (P<0.05). Moreover, calpain-2 and LC3 were mainly localized in the cytoplasm, and the co-expression rate of calpain-2 and LC3 in the NS group was higher compared with that in the sham group (P<0.05). However, the co-expression rate of calpain-2 and LC3 in the MDL-h group was significantly lower compared with that in the NS group (P<0.05; Fig. 6A-D).

Discussion

In the present study, esophageal electrical stimulation was used to establish a CA and CPR rat model. The results showed that the administration of the calpain inhibitor MDL28170 reduced pathological damage and improved the neural function by inhibiting calpain-2 (Fig. 7); it further inhibited inflammation and reduced autophagy level, reflecting a potential relationship between calpain-2 and autophagy in CIRI.

MDL28170 had no significant effect on the protein expression levels of calpain-1 and calpastatin, but had a significant inhibitory effect on the protein expression level of calpain-2 and a neuroprotective effect. Calpain-1 and calpain-2 are the two most common subtypes of calpain in the brain tissue, but there are some differences between them. Although calpain-1 and calpain-2 share a small subunit (CAPNS1) in their structures, they have completely different large subunits (32). According to the demand for calcium, calpain-1 and calpain-2 are activated by intracellular calcium at the micromole and millimole levels, respectively (33). A number of studies have shown differences in the effects of calpain-1 and calpain-2 in brain injury models. For example, calpain-1 induces heat shock protein 70 dysfunction and lysosomal membrane destruction, resulting in delayed neuronal death after transient global cerebral ischemia (34). Furthermore, another CIRI study indicated that calpain-2, rather than calpain-1, participates in the hydrolysis of the cytoskeleton protein and destroys tissue structure, consequently aggravating nerve injury (35). The present study found that MDL28170 inhibited calpain-2, rather than calpain-1, to prevent neuronal death. In line with these results, a previous study showed that MDL28170 attenuates neuronal abnormalities in rats with motor nerve damage by inhibiting calpain-2 (36), and a central nervous system development study indicated a more intimate relationship between calpain-1 and calpastatin, but calpain-2 resulted in different effects (37). These results suggest that calpain-2 induces neuronal injury, and inhibition of calpain-2 without affecting calpastatin and calpain-1 has a neuroprotective function.

TNF-α and IL-1β are common pro-inflammatory cytokines involved in neuroinflammatory responses. TNF-α is synthesized by macrophages, and its overexpression can lead to the activation of neutrophils and lymphocytes as well as the recruitment of adhesion factors, prompting the occurrence

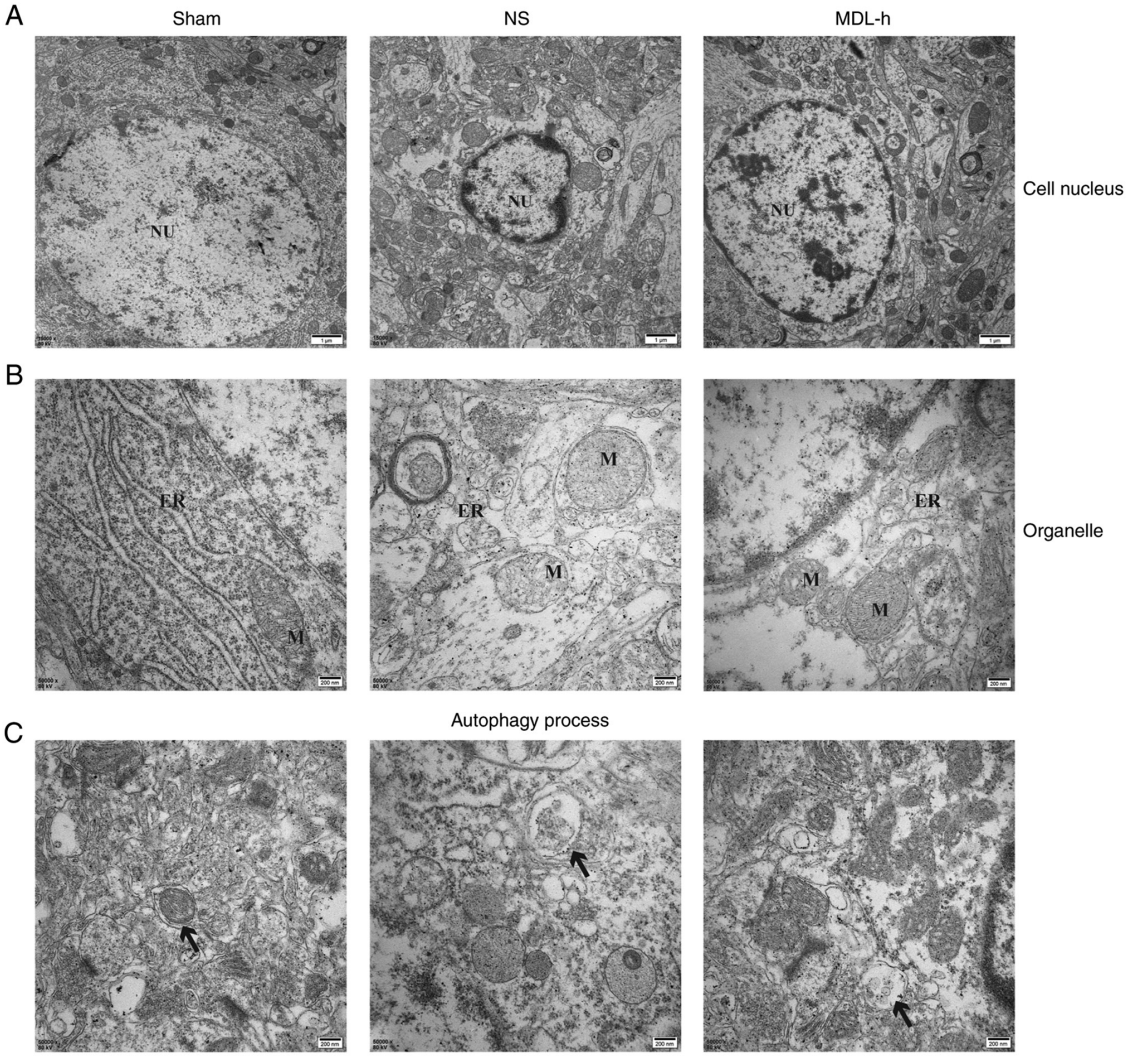

Figure 4. TEM of the cerebral cortex in rats 24 h post-CA/CPR. (A) TEM of the cell NU of neurons. The NU was intact in each group, but the size of the NU changed in the NS and MDL-h group. (B) TEM of organelle of neurons; the ER and M were damaged in the NS and MDL-h groups. (C) TEM of the autophagy process. A different feature of autophagosomes (black arrow) can be detected in the NS group. Scale bar of the first panel, 1 μm; scale bar of the second and third panels, 200 nm. (n=3). TEM, transmission electron microscopy; NU, nucleus; ER, endoplasmic reticulum; M, mitochondria; NS, normal saline; MDL-h, high-dose MDL28170 group.

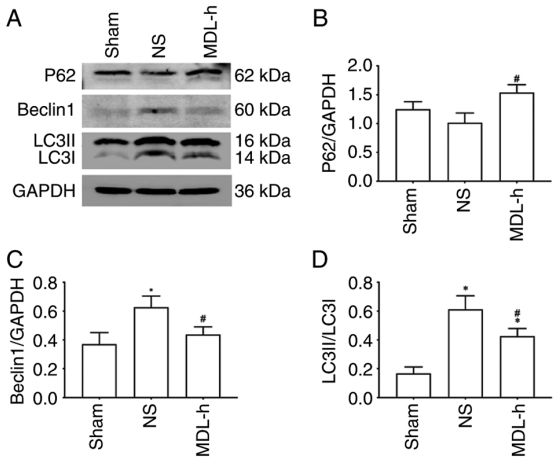

Figure 5. Western blotting for P62, beclin-1 and LC3. (A) Representative western blots of P62, beclin-1 and LC3. (B) Western blotting analysis of P62. (C) Western blotting analysis of beclin-1. (D) Western blotting analysis of LC3II/LC3I. Band intensities were normalized to those of GAPDH. (n=3). *P<0.05 vs. the sham group; #P<0.05 vs. the NS group. NS, normal saline; MDL-h, high-dose MDL28170 group.

of inflammatory reactions, and then aggravating ischemic brain tissue damage (38). The inactive precursor proIL-1β has a molecular weight 31 kDa, and matures to IL-1β with a molecular weight 17 kDa due to caspase 1 during acute injury (39). The endogenous secretion occurs rapidly, produces an inflammatory response and aggravates cell damage; thus, it is the mature IL-1β instead of the proIL-1β molecule that participates in the inflammatory response (39). The present study found that the expression of TNF-α and mature IL-1β in the cerebral cortex significantly increased after cardiopulmonary resuscitation, suggesting that the inflammatory response was involved in CIRI. MDL28170 inhibited calpain-2 in the cerebral cortex and downregulated the expression of TNF-α and mature IL-1β, suggesting that calpain-2 is potentially related to inflammation. Chen *et al* (40) showed that there is a close relationship between calpain and immune cells (especially macrophages, neutrophils and lymphocytes), and that calpain can promote the immune response when immune cells are induced. Therefore, upon the use of MDL28170 after cerebral ischemia, calpain-2 may be blocked at the same time

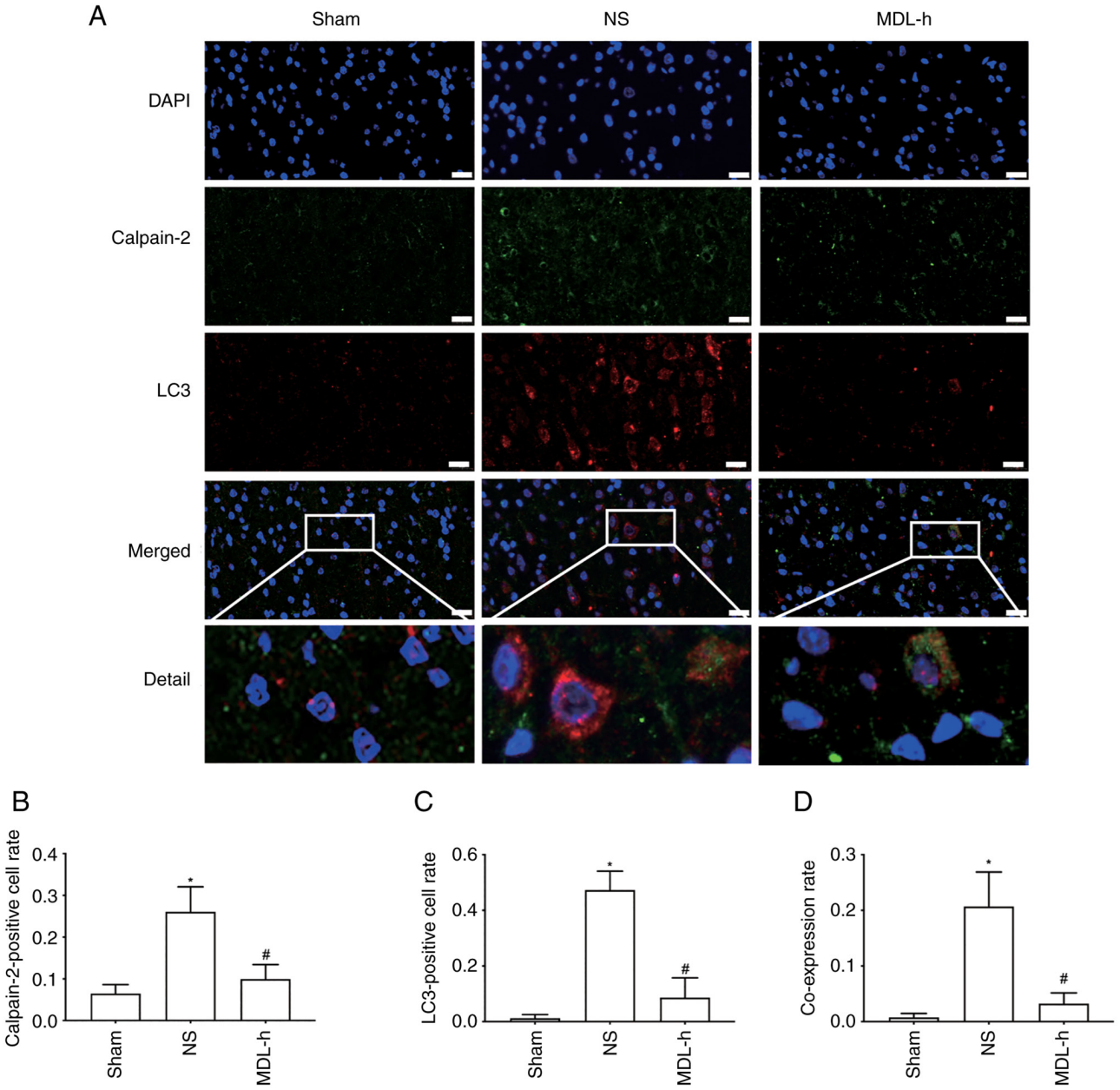

Figure 6. Double immunofluorescence staining. (A) Dual-immunofluorescence for calpain-2 and LC3 in the cerebral cortex 24 h post- cardiac arrest/cardiopulmonary resuscitation. LC3 positive cells were stained red. Calpain-2 positive cells were stained green. The nucleus was stained using DAPI (blue). Scale bar, 20 μm (white bar). The white frame in merge images are enlarged into detail images (enlarge to 4x the original image size). (B) Calpain-2-positive cell rate in groups (calpain-2-positive cell number/DAPI-positive cell number). (C) LC3-positive cell rate in groups (LC3-positive cell number/DAPI-positive cell number). (D) Calpain-2 + LC3-positive cell rate in groups (calpain-2 + LC3-positive cell number/DAPI-positive cell number). (n=3). *P<0.05 vs. the sham group; $^{\#}$P<0.05 vs. the NS group. NS, normal saline; MDL-h, high-dose MDL28170 group.

to suppress the immune response of related immune cells, thereby reducing the release of pro-inflammatory cytokines.

The accumulation of autophagosomes and damaged organelles in the cortex was observed using TEM, indicating the involvement of autophagy in CIRI after CA/CPR. In the present study, MDL28170 was found to upregulate P62 and downregulate beclin-1 and LC3I/LC3II. Moreover, double immunofluorescence staining indicated that the fluorescence signals produced by LC3 expression were present in the cytoplasm and partially co-expressed with calpain-2, which revealed a potential relationship between calpain-2 and autophagy. During CIRI, the ER and mitochondrial membrane are damaged, resulting in a dynamic imbalance in calcium concentration and calcium overload (41). Furthermore, the accumulation of certain proteins, such as calpain, induces ER stress (42), which can lead to the induction of autophagy degrade abnormally folded proteins (43-47). Autophagy is regulated by autophagy-specific genes (ATGs), including beclin-1, which is involved in the initial stages during the formation of double-membrane structures and is required for autophagosome formation (48). Additionally, during autophagy, LC3 is converted to LC3I by ATG4, followed by conjugation with phosphatidylethanolamine to form LC3II. Subsequently, P62 in the cytoplasm binds to LC3II on the membrane of the autophagosome to form a complex that is degraded by lysosomes (49,50). Thus, both p62 and LC3 are routinely used as biomarkers

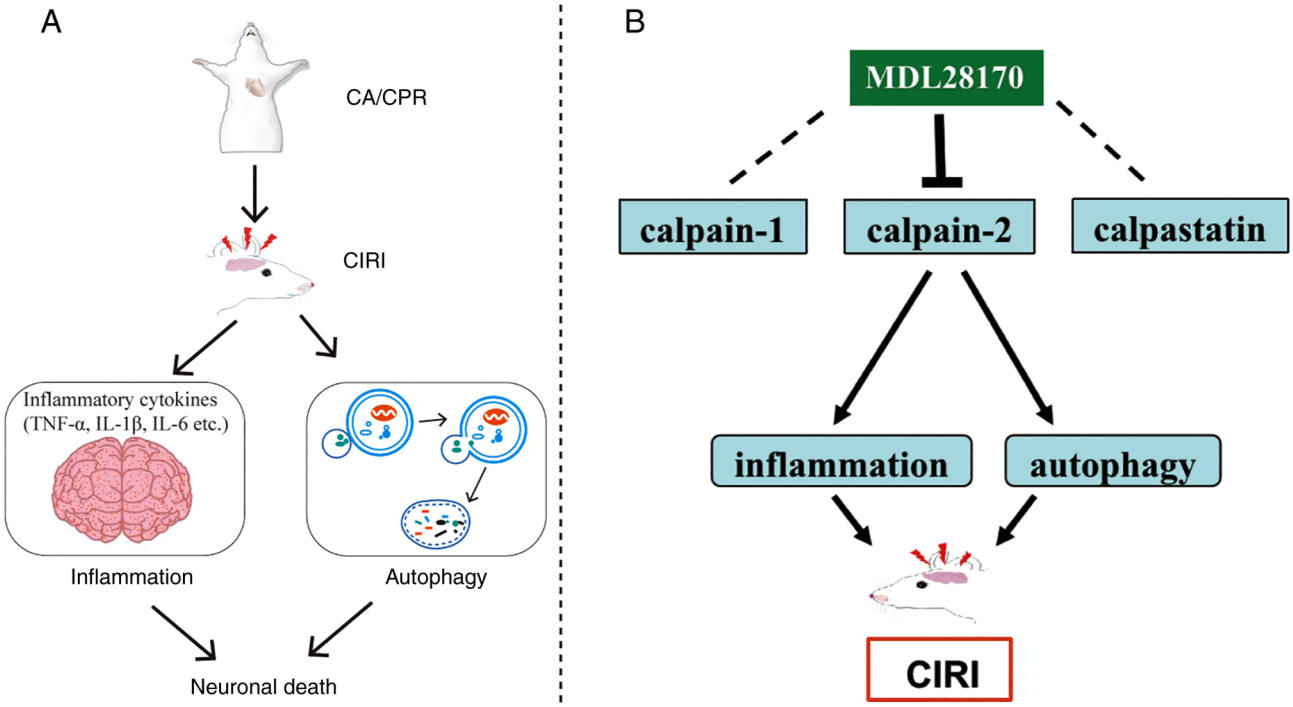

Figure 7. Graph abstract. (A) CA/CPR can induce CIRI and activate inflammation and autophagy. (B) Calpain inhibitor MDl28170 suppressed calpain-2 and improved CIRI by allieviating inflammation and autophagy in a rat model of CA. CA, cardiac arrest; CPR, cardiopulmonary resuscitation; CIRI, cerebral ischaemia reperfusion injury. TNF-α, tumour necrosis factor-a; IL-1β, interleukin 1β; IL-6, interleukin 1.

to monitor the level of autophagy (51). Autophagy acts as a cellular defense mechanism during the early stage of injury. However, excessive autophagy can promote cell death (52). Our previous research indicated that the inhibition of autophagy can ameliorate nerve functioning and play a neuroprotective role (53). In the present study, TEM showed improvements in the ER and mitochondria structures after MDL28170 administration, indicating the benefit of inhibiting autophagy by blocking calpain-2 activity, which might be related to the inhibition of calpain-2-mediated ER stress (54,55). Similar to the present results, Li *et al* (28) found that the autophagy of hippocampal neurons induced by TNF-α are mediated by calpain-2 activation, and selective calpain-2 inhibitors (calpain inhibitor IV and NA101) and calpain-2 knockout can attenuate autophagy induced by TNF-α, whereas calpain-1 knockout and inhibition resulted in no such effect. By contrast, another study showed that calpain-2 inhibition or calpain-2 knockout can enhance autophagy and reduce cell death after hepatic ischemia-reperfusion injury (56). Furthermore, Liu *et al* (57) showed that calpain-1-mediated impairment of autophagic flux contributes to cerebral ischemia-induced neuronal damage, and that MDL28170 can inhibit calpain-1 to reduce the expression of beclin-1 and ATG-5, inhibit autophagosome formation and ultimately attenuating brain damage. Therefore, the present study speculated that the relationship between calpains and autophagy depends on the degree of brain damage and activation, and the differences between models and organs.

Currently, to the best of our knowledge, there are few reports on calpains and cerebral ischemic injury induced by cardiac arrest. The most critical innovation of the present study is that it observed and compared the effects of different subtypes of calpains on brain injury induced by cardiopulmonary resuscitation in cases of cardiac arrest from different levels (pathological changes and expression of molecular proteins). Furthermore, the present study has a few limitations. First, in terms of time points, although MDL28170 showed a neuroprotective effect at 24 h after CIRI, an understanding of its long-term effect on nerve injury would be beneficial, and this requires further exploration at 48 or 72 h. Second, the side-effects of MDL28170 on the liver or kidney were not observed. Third, upstream and downstream factors of inflammation were presented via western blotting and double immunofluorescence staining. In the future, RT-qPCR is planned to be performed to verify the changes in gene expression and explore the effects of different drug concentrations. Moreover, in terms of pathophysiological mechanisms, as calcium overload can activate calpain, the evaluation of the effects of calcium-channel blockers would provide additional insight into the role of calcium in the pathophysiological mechanism.

In summary, calpain-2 activation, inflammation, and autophagy were found to be involved in CIRI after CA and CPR. Blocking calpain-2 activation with MDL28170 can significantly reduce inflammation and autophagy, which plays a neuroprotective role. These observations may help develop new strategies for treating nerve injury in patients with CA.

Acknowledgements

Not applicable.

Funding

This work was supported by the National Natural Science Foundation of China (grant nos. 81660312 and 81860333).

Availability of data and materials

All data generated or analyzed during this study are included in this published article.

Authors' contributions

WW and JS were responsible for the conceptualization, methodology, analyzing and interpreting the data, and writing of the original draft. JS was responsible for writing, reviewing and editing and funding acquisition. XZ and CD were responsible for acquiring, analyzing and interpreting the data. MC was responsible for the methodology, software and funding acquisition. LX was responsible for the conceptualization, methodology, reviewing and funding acquisition. WW and LX confirm the authenticity of all the raw data. All authors read and approved the final manuscript.

Ethics approval and consent to participate

All animal procedures were conducted in compliance with the Guide for the Care and Use of Experimental Animals. The study was approved by the Animal Ethics Committee of Guangxi Medical University (Nanning, China; approval no. 20190915).

Patient consent for publication

Not applicable.

Competing interests

The authors declare that they have no competing interests.

References

1. Andersen LW, Holmberg MJ, Berg KM, Donnino MW and Granfeldt A: In-hospital cardiac arrest: A review. JAMA 321: 1200-1210, 2019.
2. Sandroni C, D'Arrigo S and Nolan JP: Prognostication after cardiac arrest. Crit Care 22: 150, 2018.
3. Moore JC, Bartos JA, Matsuura TR and Yannopoulos D: The future is now: Neuroprotection during cardiopulmonary resuscitation. Curr Opin Crit Care 23: 215-222, 2017.
4. Goodfellow MJ, Borcar A, Proctor JL, Greco T, Rosenthal RE and Fiskum G: Transcriptional activation of antioxidant gene expression by Nrf2 protects against mitochondrial dysfunction and neuronal death associated with acute and chronic neurodegeneration. Exp Neurol 328: 113247, 2020.
5. Chen H, Yoshioka H, Kim GS, Jung JE, Okami N, Sakata H, Maier CM, Narasimhan P, Goeders CE and Chan PH: Oxidative stress in ischemic brain damage: Mechanisms of cell death and potential molecular targets for neuroprotection. Antioxid Redox Signal 14: 1505-1517, 2011.
6. Liu J, Liu MC and Wang KKW: Calpain in the CNS: from synaptic function to neurotoxicity. Sci Signal 1: re1, 2008.
7. Curcio M, Salazar IL, Mele M, Canzoniero LMT and Duarte CB: Calpains and neuronal damage in the ischemic brain: The Swiss knife in synaptic injury. Prog Neurobiol 143: 1-35, 2016.
8. Martinez JA, Zhang Z, Svetlov SI, Hayes RL, Wang KK and Larner SF: Calpain and caspase processing of caspase-12 contribute to the ER stress-induced cell death pathway in differentiated PC12 cells. Apoptosis 15: 1480-1493, 2010.
9. Sanganalmath SK, Gopal P, Parker JR, Downs RK, Parker JC Jr and Dawn B: Global cerebral ischemia due to circulatory arrest: Insights into cellular pathophysiology and diagnostic modalities. Mol Cell Biochem 426: 111-127, 2017.
10. Dókus LE, Yousef M and Bánóczi Z: Modulators of calpain activity: Inhibitors and activators as potential drugs. Expert Opin Drug Discov 15: 471-486, 2020.
11. Baudry M and Bi X: Calpain-1 and calpain-2: The yin and yang of synaptic plasticity and neurodegeneration. Trends Neurosci 39: 235-245, 2016.
12. Cheng SY, Wang SC, Lei M, Wang Z and Xiong K: Regulatory role of calpain in neuronal death. Neural Regen Res 13: 556-562, 2018.
13. Wang Y, Bi X and Baudry M: Calpain-2 as a therapeutic target for acute neuronal injury. Expert Opin Ther Targets 22: 19-29, 2018.
14. Jiao W, McDonald DQ, Coxon JM and Parker EJ: Molecular modeling studies of peptide inhibitors highlight the importance of conformational prearrangement for inhibition of calpain. Biochemistry 49: 5533-5539, 2010.
15. Betts R, Weinsheimer S, Blouse GE and Anagli J: Structural determinants of the calpain inhibitory activity of calpastatin peptide B27-WT. J Biol Chem 278: 7800-7809, 2003.
16. Potz BA, Abid MR and Sellke FW: Role of calpain in pathogenesis of human disease processes. J Nat Sci 2: e218, 2016.
17. Hu J, Chen L, Huang X, Wu K, Ding S, Wang W, Wang B, Smith C, Ren C, Ni H, *et al*: Calpain inhibitor MDL28170 improves the transplantation-mediated therapeutic effect of bone marrow-derived mesenchymal stem cells following traumatic brain injury. Stem Cell Res Ther 10: 96, 2019.
18. Thompson SN, Carrico KM, Mustafa AG, Bains M and Hall ED: A pharmacological analysis of the neuroprotective efficacy of the brain- and cell-permeable calpain inhibitor MDL-28170 in the mouse controlled cortical impact traumatic brain injury model. J Neurotrauma 27: 2233-2243, 2010.
19. Chen LN, Yan B, Chen DP and Yao YJ: Protective effect of calpain inhibitor-3 on hypoxic-ischemic brain damage of neonatal rats. Zhonghua Er Ke Za Zhi 46: 13-17, 2008 (In Chinese).
20. Li PA, Howlett W, He QP, Miyashita H, Siddiqui M and Shuaib A: Postischemic treatment with calpain inhibitor MDL 28170 ameliorates brain damage in a gerbil model of global ischemia. Neurosci Lett 247: 17-20, 1998.
21. Ravindran S and Kurian GA: Eventual analysis of global cerebral ischemia-reperfusion injury in rat brain: A paradigm of a shift in stress and its influence on cognitive functions. Cell Stress Chaperones 24: 581-594, 2019.
22. Tuttolomondo A, Di Raimondo D, Pecoraro R, Arnao V, Pinto A and Licata G: Inflammation in ischemic stroke subtypes. Curr Pharm Des 18: 4289-4310, 2012.
23. Tao XG, Shi JH, Hao SY, Chen XT and Liu BY: Protective effects of calpain inhibition on neurovascular unit injury through downregulating nuclear factor-κB-related inflammation during traumatic brain injury in mice. Chin Med J (Engl) 130: 187-198, 2017.
24. Wang WY, Xie L, Zou XS, Li N, Yang YG, Wu ZJ, Tian XY, Zhao GY and Chen MH: Inhibition of extracellular signal-regulated kinase/calpain-2 pathway reduces neuroinflammation and necroptosis after cerebral ischemia-reperfusion injury in a rat model of cardiac arrest. Int Immunopharmacol 93: 107377, 2021.
25. Edinger AL and Thompson CB: Death by design: Apoptosis, necrosis and autophagy. Curr Opin Cell Biol 16: 663-669, 2004.
26. Ashrafi G and Schwarz TL: The pathways of mitophagy for quality control and clearance of mitochondria. Cell Death Differ 20: 31-42, 2013.
27. Zheng JH, Xie L, Li N, Fu ZY, Tan XF, Tao R, Qin T and Chen MH: PD98059 protects the brain against mitochondrial-mediated apoptosis and autophagy in a cardiac arrest rat model. Life Sci 232: 116618, 2019.
28. Li Y, He Z, Lv H, Chen W and Chen J: Calpain-2 plays a pivotal role in the inhibitory effects of propofol against TNF-α-induced autophagy in mouse hippocampal neurons. J Cell Mol Med 24: 9287-9299, 2020.
29. Chen MH, Liu TW, Xie L, Song FQ, He T, Zeng ZY and Mo SR: Ventricular fibrillation induced by transoesophageal cardiac pacing: a new model of cardiac arrest in rats. Resuscitation 74: 546-551, 2007.
30. Du PR, Lu HT, Lin XX, Wang LF, Wang YX, Gu XM, Bai XZ, Tao K and Zhou JJ: Calpain inhibition ameliorates scald burn-induced acute lung injury in rats. Burns Trauma 6: 28, 2018.
31. Jia X, Koenig MA, Shin HC, Zhen G, Pardo CA, Hanley DF, Thakor NV and Geocadin RG: Improving neurological outcomes post-cardiac arrest in a rat model: Immediate hypothermia and quantitative EEG monitoring. Resuscitation 76: 431-442, 2008.

32. Cataldo F, Peche LY, Klaric E, Brancolini C, Myers MP, Demarchi F and Schneider C: CAPNS1 regulates USP1 stability and maintenance of genome integrity. Mol Cell Biol 33: 2485-2496, 2013.
33. Zheng P, Chen X, Xie J, Chen X, Lin S, Ye L, Chen L, Lin J, Yu X and Zheng M: Capn4 is induced by and required for Epstein-Barr virus latent membrane protein 1 promotion of nasopharyngeal carcinoma metastasis through ERK/AP-1 signaling. Cancer Sci 111: 72-83, 2020.
34. Zhu H, Yoshimoto T, Imajo-Ohmi S, Dazortsava M, Mathivanan A and Yamashima T: Why are hippocampal CA1 neurons vulnerable but motor cortex neurons resistant to transient ischemia? J Neurochem 120: 574-585, 2012.
35. Fukuda S, Harada K, Kunimatsu M, Sakabe T and Yoshida K: Postischemic reperfusion induces alpha-fodrin proteolysis by m-calpain in the synaptosome and nucleus in rat brain. J Neurochem 70: 2526-2532, 1998.
36. Zang Y, Chen SX, Liao GJ, Zhu HQ, Wei XH, Cui Y, Na XD, Pang RP, Xin WJ, Zhou LJ and Liu XG: Calpain-2 contributes to neuropathic pain following motor nerve injury via up-regulating interleukin-6 in DRG neurons. Brain Behav Immun 44: 37-47, 2015.
37. Li Y, Bondada V, Joshi A and Geddes JW: Calpain 1 and calpastatin expression is developmentally regulated in rat brain. Exp Neurol 220: 316-319, 2009.
38. Xiong XY, Liu L and Yang QW: Functions and mechanisms of microglia/macrophages in neuroinflammation and neurogenesis after stroke. Prog Neurobiol 142: 23-44, 2016.
39. Lopez-Castejon G and Brough D: Understanding the mechanism of IL-1β secretion. Cytokine Growth Factor Rev 22: 189-195, 2011.
40. Chen Y, Su Z and Liu F: Effects of functionally diverse calpain system on immune cells. Immunol Res 69: 8-17, 2021.
41. Guo MM, Qu SB, Lu HL, Wang WB, He ML, Su JL, Chen J and Wang Y: Biochanin A alleviates cerebral ischemia/reperfusion injury by suppressing endoplasmic reticulum stress-induced apoptosis and p38MAPK signaling pathway in vivo and in vitro. Front Endocrinol (Lausanne) 12: 646720, 2021.
42. Thompson J, Maceyka M and Chen Q: Targeting ER stress and calpain activation to reverse age-dependent mitochondrial damage in the heart. Mech Ageing Dev 192: 111380, 2020.
43. Li W, Zhu J, Dou J, She H, Tao K, Xu H, Yang Q and Mao Z: Phosphorylation of LAMP2A by p38 MAPK couples ER stress to chaperone-mediated autophagy. Nat Commun 8: 1763, 2017.
44. Lépine S, Allegood JC, Edmonds Y, Milstien S and Spiegel S: Autophagy induced by deficiency of sphingosine-1-phosphate phosphohydrolase 1 is switched to apoptosis by calpain-mediated autophagy-related gene 5 (Atg5) cleavage. J Biol Chem 286: 44380-44390, 2011.
45. So KY, Lee BH and Oh SH: The critical role of autophagy in cadmium-induced immunosuppression regulated by endoplasmic reticulum stress-mediated calpain activation in RAW264.7 mouse monocytes. Toxicology 393: 15-25, 2018.
46. Demarchi F, Bertoli C, Copetti T, Tanida I, Brancolini C, Eskelinen EL and Schneider C: Calpain is required for macroautophagy in mammalian cells. J Cell Biol 175: 595-605, 2006.
47. Li XY, Meng L, Wang F, Hu XJ and Yu YC: Sodium fluoride induces apoptosis and autophagy via the endoplasmic reticulum stress pathway in MC3T3-E1 osteoblastic cells. Mol Cell Biochem 454: 77-85, 2019.
48. Qu X, Yu J, Bhagat G, Furuya N, Hibshoosh H, Troxel A, Rosen J, Eskelinen EL, Mizushima N, Ohsumi Y, *et al*: Promotion of tumorigenesis by heterozygous disruption of the beclin 1 autophagy gene. J Clin Invest 112: 1809-1820, 2003.
49. Glick D, Barth S and Macleod KF: Autophagy: Cellular and molecular mechanisms. J Pathol 221: 3-12, 2010.
50. Kaur J and Debnath J: Autophagy at the crossroads of catabolism and anabolism. Nat Rev Mol Cell Biol 16: 461-472, 2015.
51. Klionsky DJ, Abdalla FC, Abeliovich H, Abraham RT, Acevedo-Arozena A, Adeli K, Agholme L, Agnello M, Agostinis P, Aguirre-Ghiso JA, *et al*: Guidelines for the use and interpretation of assays for monitoring autophagy. Autophagy 8: 445-544, 2012.
52. Gustafsson AB and Gottlieb RA: Autophagy in ischemic heart disease. Circ Res 104: 150-158, 2009.
53. Nguyen Thi PAN, Chen MH, Li N, Zhuo XJ and Xie L: PD98059 protects brain against cells death resulting from ROS/ERK activation in a cardiac arrest rat model. Oxid Med Cell Longev 2016: 3723762, 2016.
54. Xie RJ, Hu XX, Zheng L, Cai S, Chen YS, Yang Y, Yang T, Han B and Yang Q: Calpain-2 activity promotes aberrant endoplasmic reticulum stress-related apoptosis in hepatocytes. World J Gastroenterol 26: 1450-1462, 2020.
55. Ly LD, Xu S, Choi SK, Ha CM, Thoudam T, Cha SK, Wiederkehr A, Wollheim CB, Lee IK and Park KS: Oxidative stress and calcium dysregulation by palmitate in type 2 diabetes. Exp Mol Med 49: e291, 2017.
56. Zhao Q, Guo Z, Deng W, Fu S, Zhang C, Chen M, Ju W, Wang D and He X: Calpain 2-mediated autophagy defect increases susceptibility of fatty livers to ischemia-reperfusion injury. Cell Death Dis 7: e2186, 2016.
57. Liu Y, Che X, Zhang H, Fu X, Yao Y, Luo J, Yang Y, Cai R, Yu X, Yang J and Zhou MS. CAPN1 (Calpain1)-mediated impairment of autophagic flux contributes to cerebral ischemia-induced neuronal damage. Stroke 52: 1809-1821, 2021.